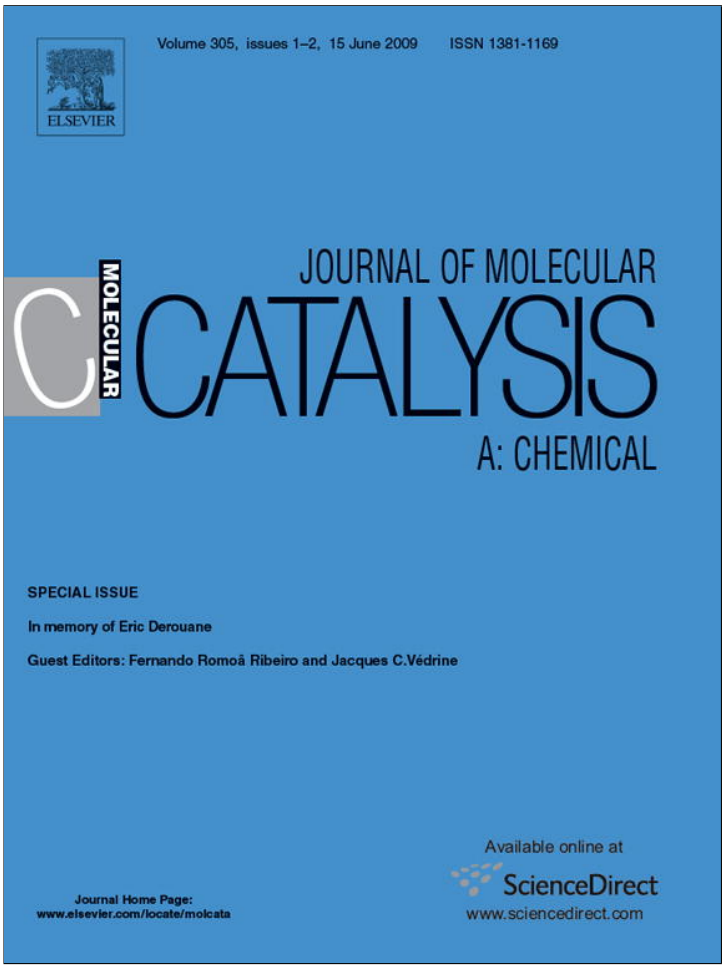

Journal of Molecular Catalysis A: Chemical 305 (2009) 16–23

Contents lists available at ScienceDirect

Journal of Molecular Catalysis A: Chemical

journal homepage: www.elsevier.com/locate/molcata

Confinement in molecular sieves: The pioneering physical concepts

A.A. Lucas[a,b], I. Derycke[a], Ph. Lambin[a], J.-P. Vigneron[a,b], L. Leherte[a], M. Elanany[a,1], J.-M. André[a,b], A.V. Larin[a], D.P. Vercauteren[a,*]

[a] University of Namur (FUNDP), Rue de Bruxelles 61, B-5000 Namur, Belgium
[b] Académie Royale de Belgique, B-1000 Bruxelles, Belgium

ARTICLE INFO

Article history:
Available online 24 March 2009

Keywords:
Adsorption energy
Confinement
Surface curvature effects
Zeolites

ABSTRACT

The activity of Prof. Eric G. Derouane expanded over numerous directions in zeolite chemistry, from the development of pioneering physical concepts to the optimization of chemical synthesis, including catalysis. His ideas were an inspiring basis of many modern experimental and theoretical studies for many researchers at the University of Namur. In this University, where Eric has been Full Professor for over 20 years, all of us have benefited from Eric's friendship and from numerous frequent and fruitful discussions in the zeolite domain. D.P.V. is particularly indebted to Eric's long term vision regarding the multiple aspects to tackle using molecular simulations of sieves in general.

With this paper, we wish to honor Eric's memory by recalling the pioneering physical concepts of confinement which have influenced more than 20 years of theoretical simulations of molecular sieves. We will also briefly mention the on-going theoretical work towards template design for the syntheses of porous materials.

1. How Eric got kick started on confinement

One of us (A.A.L.) vividly remembers when we got started with confinement. Here is his short account of what happened:

> "It was in June 1986, while I was boring away undergraduate oral exams in the summer heat of a classroom, when I received from Eric a short note written on a scratch of paper. I welcomed the distraction and got immediately interested by what Eric was asking:
>
> "Amand, do you know how to evaluate the adsorption energy of a molecule in a small cavity of a solid?". I knew what Eric had in mind given his passion for catalysis and zeolites in which reacting molecules are tightly confined to atomically narrow pores. Eric must have thought that he'd better ask the "local expert" in van der Waals (vdW) forces. Indeed, ten years earlier I happened to have worked, with a Ph.D. student, Marcel Schmeits of the University of Liège, on a general theory of physisorption on curved, convex or concave surfaces [1]. I did remember by heart the formula for the simple case of physisorption of an isotropic molecule in a spherical cavity in a perfect metallic continuum. The attractive part of the adsorption energy is given by the simple rational function:

$$W(s) = -\left(\frac{C}{4d^3}\right)\left(1-\frac{s}{2}\right)^{-3} \quad (1)$$

> with the ratio $s = d/a$ where d is the adsorption distance to the pore wall of radius a and C/d^3 is the flat surface value.
>
> I sent this formula to Eric with a few comments on the back of the proverbial envelope, pointing out that for $s = 1$ (tight fit), the adsorption energy could be an order of magnitude (8 times) larger than the flat surface value, while the sticking force would vanish.
>
> Eric called me back, enormously excited asking whether I realized how important this was for zeolite chemistry. I said "No, but I do believe you".

This is how a brief but very intense collaboration started on this subject between Eric and myself, along with a few other theoreticians in Namur [2–9]".

2. The basic idea

Fig. 1 ought to convey the basic argument of confinement. Considering only the vdW attractive part of the adsorption energy of a molecule on a surface and assuming additivity of the interatomic forces, the (negative) adsorption energies on a concave,

* Corresponding author. Tel.: +32 81 72 45 34; fax: +32 81 72 54 66.
E-mail address: daniel.vercauteren@fundp.ac.be (D.P. Vercauteren).
[1] FNRS Post-Doctoral Research Fellow.

1381-1169/$ – see front matter © 2009 Elsevier B.V. All rights reserved.
doi:10.1016/j.molcata.2009.02.040

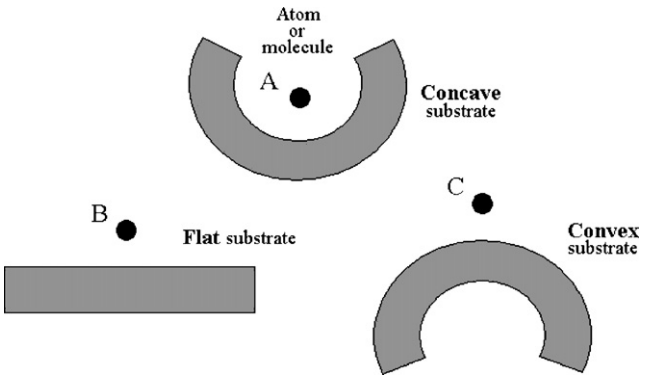

Fig. 1. Principle of confinement (A) and anti-confinement (C).

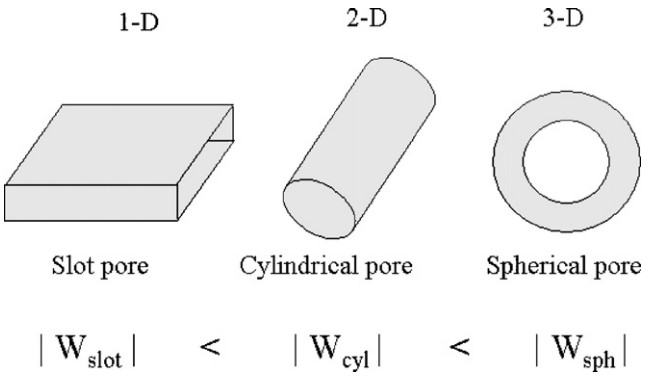

Fig. 2. Dimensionality effect on confinement.

flat or convex surface should order as $|W_{concave}|>|W_{flat}|>|W_{convex}|$, merely on account of the number of nearest neighbors of the adsorbate in the three cases. The (positive) repulsion energies weaken somewhat this argument but do not invalidate it since attraction dominates repulsion and has longer range.

Fig. 2 provides another kind of ordering, which depends on the dimensionality of the confining cavity. Again the adsorption energies tend to be larger the stronger the confinement, i.e., in pores of higher dimensions.

One can obtain a rough idea of the confinement effect in 3-D by treating the substrate as a continuum interacting with the adsorbate via a r^{-n} power law (Fig. 3a):

$$W_{sphere} = -\int_a^\infty d\vec{r}\,\frac{A}{r^n} = -\frac{4\pi A}{(n-3)a^3}$$

where A is a constant.

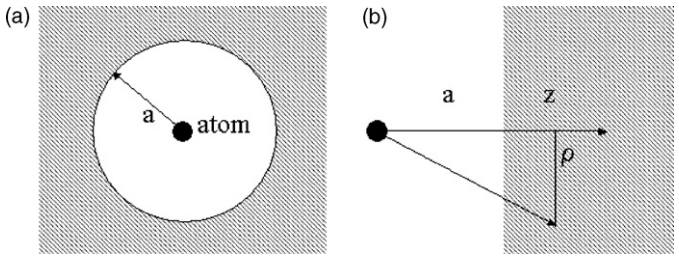

Fig. 3. Scheme for the calculation of the adsorption at the centre of a spherical pore (a) compared to a flat surface (b).

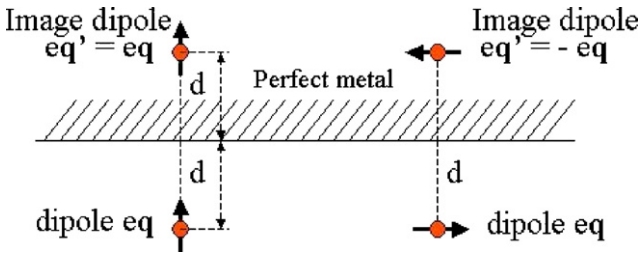

Fig. 4. Image dipole of an object dipole in normal (a) or parallel (b) orientations to a flat surface.

Similarly, for a flat substrate (Fig. 3b):

$$W_{flat} = -\int d\vec{r}\,\frac{A}{(z^2+\rho^2)^{n/2}} = -\frac{2\pi A}{(n-2)(n-3)a^{n-3}}$$
$$= W_{sphere}/2(n-2)$$

For the vdW exponent $n=6$, one sees that $W_{sphere} = 8\,W_{flat}$, which is the result from the general formula (1) for $s=1$ and $d=a$.

This spectacular effect, which appears to have been pointed out by de Boer and Custers [10] long ago, was what struck Eric who immediately thought of its potential consequences for catalysis in molecular sieves in general and zeolite pores in particular. Notice that the confinement effect is even more pronounced for the repulsion part of the adsorption energy: e.g., for the Lennard–Jones repulsion exponent $n=12$, $W_{sphere} = 20\,W_{flat}$.

3. Image methods

3.1. Flat surface

Here we wish to re-derive Eq. (1) in an elementary manner. Only quantum mechanics allows to understand the truly quantum nature and origin of the dispersion forces in physisorption. However the image charge method of classical electrodynamics in the quasi-static approximation (electrostatics) does provide a convenient, illuminating approach to the problem, the quantum being introduced only at the end of the calculations.

Let us first apply the image method to the vdW energy of an atom at a distance d from the flat surface of a perfect metallic continuum (Fig. 4). The atom is viewed as a point dipole moment $e\boldsymbol{q}$ harmonically fluctuating at the free frequency ω; the metal substrate responds by producing a synchronously fluctuating image dipole $e\boldsymbol{q}'$ symmetrically placed at distance d from the surface. Note that $e\boldsymbol{q}' = e\boldsymbol{q}$ or $-e\boldsymbol{q}$ according to whether the oscillation is perpendicular (Fig. 4a) or parallel to the surface (Fig. 4b), respectively.

The instantaneous (non-retarded) interaction energy of the object dipole with its image dipole is given by:

$$V = \left(\frac{1}{2}\right) e\boldsymbol{q}\cdot\left\{\frac{1-3\boldsymbol{d}^0\boldsymbol{d}^0}{(2d)^3}\right\}\cdot e\boldsymbol{q}' \qquad (2)$$

where $\boldsymbol{d}^0 = \boldsymbol{d}/d$ is the unit vector perpendicular to the surface and where the extra factor 1/2 arises from the induced nature of the image. Introducing this interaction term in the Hamiltonian of the atomic oscillator, one finds that it has the following downward shifted frequencies:

$$\omega_\perp = \omega\left(1-\frac{\alpha}{4d^3}\right)^{1/2} \quad \text{(single mode)} \qquad (3)$$

$$\omega_{||} = \omega\left(1-\frac{\alpha}{8d^3}\right)^{1/2} \quad \text{(twice degenerate mode)} \qquad (4)$$

where $\alpha = e^2/m\omega^2$ is the static dipole polarizability of the atom.

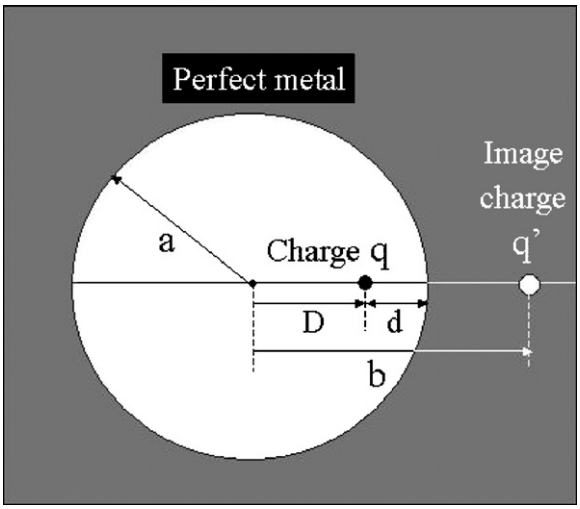

Fig. 5. Image charge q' of an object charge q in a spherical pore.

Now comes the quantum mechanical step. Upon removing the atom from d to infinity, the London dispersion energy is the ***shift of zero-point energy*** of the system:

$$W_{\text{flat}} = \left(\frac{1}{2}\right)\hbar(\omega_{\perp} + \omega_{||} - 3\omega) \tag{5}$$

This is an ***exact result*** for the present model system [7]. Expanding the square roots in (3) and (4) in powers of $\alpha/4d^3$, one finds ***to lowest order in*** α:

$$W_{\text{flat}} = -\left(\frac{1}{2}\right)\hbar\omega\left(\frac{\alpha}{4d^3}\right) \tag{6}$$

which is the familiar power law for the non-retarded vdW interaction of an atom with a semi-infinite substrate.

3.2. Spherical pore

Let us suppose that a point charge q is placed inside a spherical cavity of radius a in a perfect metal (Fig. 5), at a distance D from the centre. A distribution of charges of opposite sign is induced on the surface of the sphere. The effect of the induced charge is equivalent to that of an image charge q' placed outside the sphere at a distance b, co-radially with q. Both q' and b can be determined by demanding that the electrical voltage be zero on the metal surface. The result is $q' = -qa/D$ and $b = a^2/D$. From this, a point dipole $\boldsymbol{p}$ placed at D induces an image dipole $\boldsymbol{p}'$ at distance b where $\boldsymbol{p}' = \boldsymbol{p}a/D$ or $-\boldsymbol{p}a/D$ depending on whether the oscillation is radial (Fig. 6a) or tangential

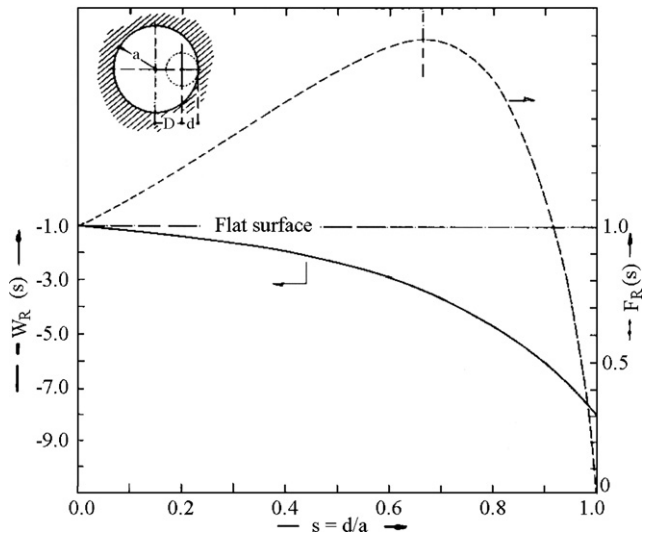

Fig. 7. Adsorption energy (left scale) and sticking force (right scale) as a function of $s = d/a$ for an atom in a spherical pore relative to the flat surface case (attraction only; reproduced from ref. [5]).

(Fig. 6b), respectively. The interaction energy is now given by:

$$V = \left(\frac{1}{2}\right)\boldsymbol{p}\cdot(E - 3\boldsymbol{d}^0\boldsymbol{d}^0)\cdot\frac{\boldsymbol{p}'}{(b-D)^3} \tag{7}$$

from which one can again obtain the shifted frequencies of the single radial and doubly degenerate tangential modes of harmonic oscillations. Expanding the frequencies in powers of α, and summing the zero point energies of all the modes as before, one finds ***to first order in powers of*** α:

$$W(s) = 2\left(\frac{C}{D^3}\right)r^3(r^2-1)^{-3} = -\left(\frac{C}{4d^3}\right)\left(1-\frac{s}{2}\right)^{-3}$$
$$= W_{\text{flat}}\left(1-\frac{s}{2}\right)^{-3} \tag{8}$$

where $C = \hbar\omega\alpha/2$, $r = D/a$, $s = 1 - r = d/a$.

Fig. 7 illustrates the behaviour of $W(s)$ for $0 < s < 1$ and the attraction force $-dW(s)/dD$ by the pore wall for fixed adsorption distance d and variable pore radius a.

4. Conclusions from the original papers

From these rather simple initial results, and although repulsion was not included in the model at the early stage, Eric was able to draw several qualitative conclusions regarding the effect of confinement on the sorption properties of microporous substrates:

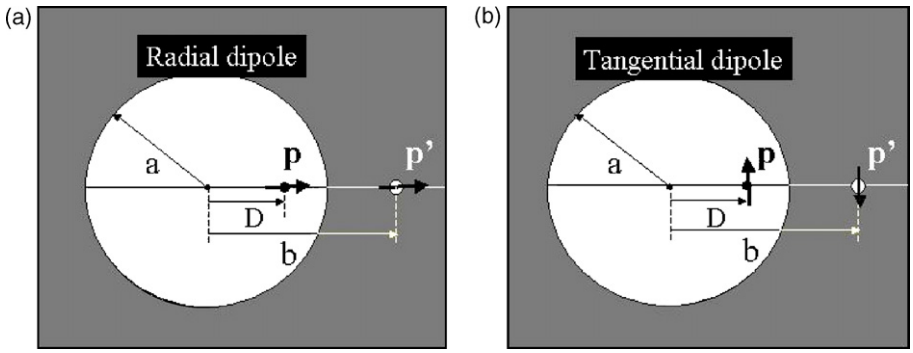

Fig. 6. Image dipole of an object dipole in radial (a) or tangential (b) orientations to a spherical pore.

(1) Increase of the (van der Waals) adsorption energy on concave surfaces;
(2) Increase of the sticking force to the pore wall for loose fit;
(3) Increase of the barrier height at the pore centre for loose fit;
(4) Vanishing of the barrier height (and the sticking force) for tight fit;
(5) Because $|W_{convex}| < |W_{concave}|$ (Fig. 1), there must exist a sorption barrier for a molecule entering a pore from an external surface.

Loose or tight fit refers here to pore sizes larger or close to the vdW radius of the adsorbate, respectively. Racing ahead in his reasoning, from point (3) Eric conjectured that in loose cylindrical pores of zeolites, the diffusion of adsorbed species might proceed by a ***creeping process along the pore wall*** rather than by exploring the entire pore space. And from point (4), he predicted, somewhat paradoxically, that there ought to be a large enhancement of diffusivity through tight pores.

5. Improvements over the simple, perfect metal substrate

The simplification of using a perfect metallic response for the substrate is likely to exaggerate the confinement effects and is hardly applicable when dealing with insulator or semiconductor substrate such as zeolitic materials. Improvements were therefore brought to the analysis in the following ways.

(1) In their earlier paper, Schmeits and Lucas [1] had treated a substrate of finite, dynamical polarizability via the use of a frequency-dependent dielectric constant $\varepsilon(\omega)$. For example, considering the adsorption of Ar in a spherical pore in Ag, they found and enhancement factor of 5.4 instead of 8 for tight fit; still a sizable enhancement;
(2) 1-D, 2-D and 3-D confinement effects (Fig. 2) were studied by Derycke et al. [9] who used a classical 6–12 Lennard–Jones (LJ) potential in the continuum approximation. Fig. 8 shows the result for 3-D adsorption, reproduced from ref. [9]. Repulsion is seen to reduce somewhat the confinement effects although, for tight fit, the enhancement factor over the flat surface adsorption energy is still more than 4. One important effect of repulsion is to shift the equilibrium adsorption distance away from the surface as compared to the flat surface value. The enhancement of the central barrier for loose fit is confirmed as well as the vanishing of the barrier for tight fit.

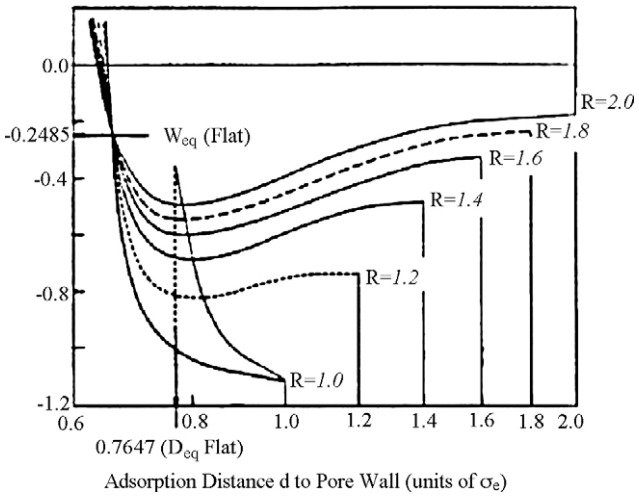

Fig. 8. Adsorption energy as a function of the distance *d* for an atom in a spherical pore for various pore radii *R* (repulsion included; reproduced from ref. [9]).

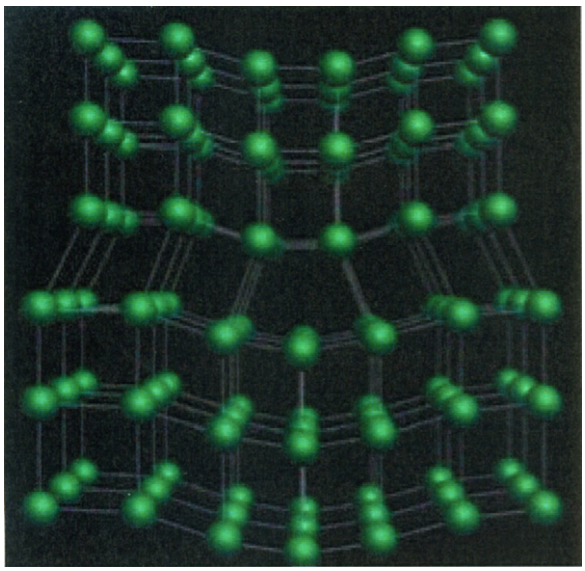

Fig. 9. 3-D view of an edge dislocation in a crystal lattice. This figure is taken from the Web page "Background Info" at http://me3007.wikidot.com/thermal-properties-of-carbon-nanotubes.

(3) Finally, departing from the continuum approximation of the previous models, Derouane et al. [8] took atomicity into account with LJ pair potentials and did confirm the expected existence of a surface barrier to sorption into cylindrical pores in a mordenite substrate.

6. Pipe diffusion: confinement in metals, ceramics, and zeolites

The enhancement of diffusion in tight pores conjectured by Eric has recently been observed in a context quite different from zeolites.

It has been known for a long time that in most solid materials – metals, alloys as well as ceramics – the jump rate of atoms is much higher along certain high-diffusivity paths than through the bulk crystalline lattice. Such paths can be grain boundaries, dislocations, free outer surfaces, inner void surfaces, interfaces, etc. . ., where the diffusing species encounter an atomic packing density reduced from its bulk lattice value. Dislocation pipe diffusion or ***pipe diffusion*** for short is the name frequently given to diffusion along dislocations. The name obviously refers to the predominantly 1-D nature of atomic jumps along this linear defect.

Fig. 9 illustrates the concept. It is a perspective view depicting an edge dislocation, i.e., an insertion of an extra plane of atoms, in a crystal lattice. One expects that interstitial host atoms or foreign atoms trapped in that kind of defect would diffuse more easily along such broader channels than along narrower lattice channels.

As an example, a recent spectacular observation and measurement of pipe diffusion has been made by Legros et al. [11] who used TEM (transmission electron microscopy) to observe and characterize the phenomenon of Oswald ripening of Si precipitates in an Al matrix. The principle of the method (Fig. 10a) was to measure visually under the microscope the rate of shrinkage of the small precipitate emptying its content into the large precipitate via a fast diffusion along the dislocation which connects them. The measured rate allowed deducing the pipe diffusion coefficient shown in Fig. 10b (adapted from ref. [11]). The measured diffusivity is several orders of magnitude higher than the bulk diffusivity at the same temperature. The diffusing Si atoms find it much easier to move along the dislocation core where they encounter a reduced atomic density. But is the enhanced jump rate consistent with the

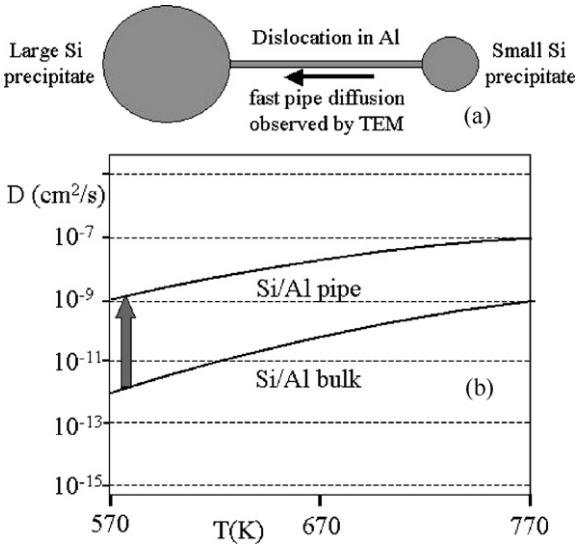

Fig. 10. (a) Oswald ripening of Si precipitates mediated by pipe diffusion in Al. (b) Pipe diffusion coefficient of Si/Al compared to bulk lattice diffusion as a function of temperature (adapted from ref. [11]).

reduction in density? In other words, will diffusivity continue to increase if the density vanishes, as the pipe diameter grows beyond the size of the diffusing species towards mesoscopic sizes?

Contrary to what one would intuitively expect, the answer appears to be the reverse, as pointed out by Eric in one of his publications wherein NMR measurements supported confinement effects [6].

Eric and collaborators made detailed comparisons of diffusion rates in ZSM-5, which presents well defined one-dimensional, pipe-like, empty channels, as well as other zeolites. To quote from Eric [6], *"A molecule may acquire supermobility when its dimensions match intimately that of the surrounding pore, a case referred to as the floating molecule. Consequently, in contrast to intuitive and qualitative reasoning, we conclude that the diffusion rate increases as the molecule and pore sizes match each other more intimately".*

7. From sorption, diffusion, and reactivity of zeolites toward their syntheses

In many later works including some recent ones [12–18], Eric continued to emphasize the subtle effects of confinements and the enhanced role of physical adsorption in the sorption, diffusion, and reactivity properties of zeolite catalysts, this in correlation with numerous experimental estimations of both static (heats of adsorption, ...) and dynamic (NMR relaxation times, sorption kinetics, diffusion coefficients, ...) properties. Several families of sorbents, alkanes, cycloalkanes, xylenes, diisopropylnaphtalenes, methylamine bases, ..., in a variety of 3-D frameworks, ZSM-5, ferrierite, mordenite, zeolite Y, zeolite L, zeolite T, AlPOs, SAPOs ..., were analyzed. Along the years and very often under Eric's proposal, a new "molecular catalysis" vocabulary, although not accepted directly in the first years, has emerged. Among other, let us cite *"surface curvature effects, window effects, structural recognition and pre-organization, molecular trapping, molecular nesting, molecular shape selectivity, molecular traffic control, floating molecule, creeping diffusion, zeolites as solid solvents, ..."*

In parallel, the theoretical chemists of the University of Namur went on to improve both the use of LJ potentials and atomistic simulations. Not widely known was the creation, in the beginning of the 1990s, of specific molecular graphics modules to tackle adsorption in 3-D frameworks [19]. The system included particular parameters of the LJ potential (depth of potential well and collision parameter, needed in the so-called combination rules) to allow studying the best shape complementarity between organic type molecules (meaning special parameters for carbons, hydrogens, for example) versus the 3-D frameworks (meaning special parameters for oxygens, silicons, aluminiums, for example, and special parameters for the capping hydrogens); these parameters were fitted from the numerous experimental evidences of the possible guest molecules inside the host frameworks (Fig. 11). This last figure depicts the straight and sinusoidal channels of ZSM-5 loaded with p-xylene molecules.

Interestingly, the graphics system also allowed to monitor in real time the interaction energy of a sorbent molecule versus all framework atoms, considered with periodic conditions (Fig. 12).

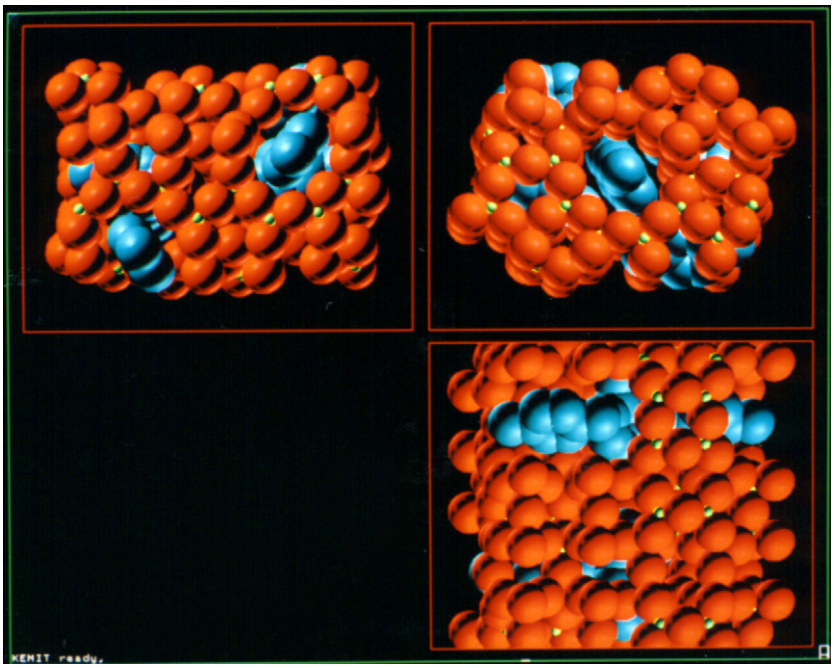

Fig. 11. Orthographic view of p-xylene molecules in both the straight and sinusoidal channels of ZSM-5. Cutting plans allow visualizing the sinusoidal channels.

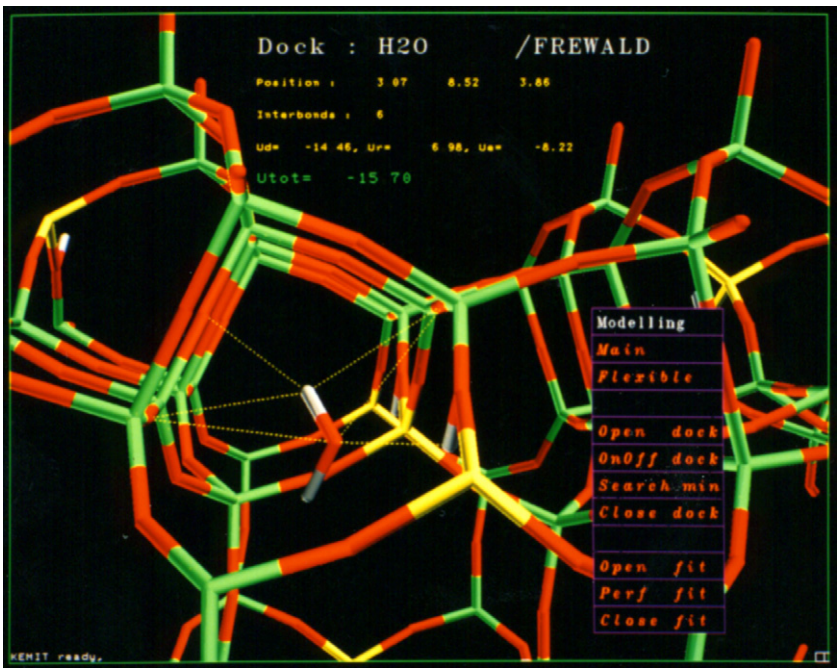

Fig. 12. View of real time monitoring of the non-bonding interaction energy between water and the periodic framework (i.e., Ewald summation) of H-ferrierite while moving water. Dotted lines depict H-bonds between water and the oxygen and hydrogen framework atoms.

The figure details the interaction – dispersion, repulsion, and electrostatic – terms as well as the total non-bonding energy while rotating and translating a water molecule inside H-ferrierite.

On the atomistic type calculations, Eric has foster, starting mainly with L.L. and D.P.V., intensive molecular statistics simulations (i.e., Monte Carlo, MC, and molecular dynamics, MD) regarding, for example, various densities of water molecules in 3-D periodical frameworks of H-ferrierite [20]. Among numerous results (radial diffusion functions, diffusion coefficients, autocorrelation functions, . . .) which were validated by corroboration with experimental results (IR, NMR, inelastic neutron scattering, . . .), the studies showed nicely how water molecules escaped from the centre of the framework cavities and formed cages of water along the zeolite walls (Fig. 13). The figure, obtained by MD simulation, shows the cage structure of the water molecules formed by H-bonds among themselves and with the walls of the H-ferrierite framework. Continuing along the road, let us also mention the numerous MC, MD, and jump diffusion simulations of butene isomers or benzene in different types of zeolite systems handled by Jousse et al. [21–23]. From their work, Fig. 14 illustrates clearly the creeping effect of a benzene molecule in zeolite HY.

It should be pointed out that electrostatic and polarization interactions may also contribute to altered adsorption energies in confined physisorption. Zeolites are partly ionic materials where charge transfers between chemical elements of the framework may result in strong local electrostatic crystal fields. Hence, polarization (or induction) and electrostatic interactions of adsorbed molecules with the zeolite framework could additionally stabilize the products of either physical or chemical adsorption. It is expected that such interactions are site-dependent as well as pore size-dependent. The main question is however whether the relative energies of adsorption or of reactions obtained regarding only vdW terms could be reordered by adding the other long range terms, i.e., electrostatic and polarization interactions with the framework.

It has been shown that vdW terms dominate in the total interaction energy values versus the electrostatic and polarization ones in several cases. It is true for polar CH_3CN (dipole of 3.11 D) [24], less polar CO (dipole of 0.03 D) [25–26], and non-polar N_2 [25–26] molecules. Examples of small relative electrostatic additions to the total energy were obtained for CH_3CN in mordenite, i.e., less than 1 kcal/mol [24], for CO, i.e., less than 2 kcal/mol in RbNaY [26] in NaCaA [25], and less than 4 kcal/mol in NaY [26]. Small polarization (induction) energies less than 1–2 kcal/mol were calculated for CO and N_2 in A [25] and Y [26] type zeolites. The role of these electrostatic and polarization terms was elucidated by adjusting the total interaction energies to ensure a good agreement between the calculated and the experimental band shift values of fundamental transition in N_2 or CO probes [25–26].

We here also wish to stress that the precise answer regarding the electrostatic and polarization contributions depend on the accu-

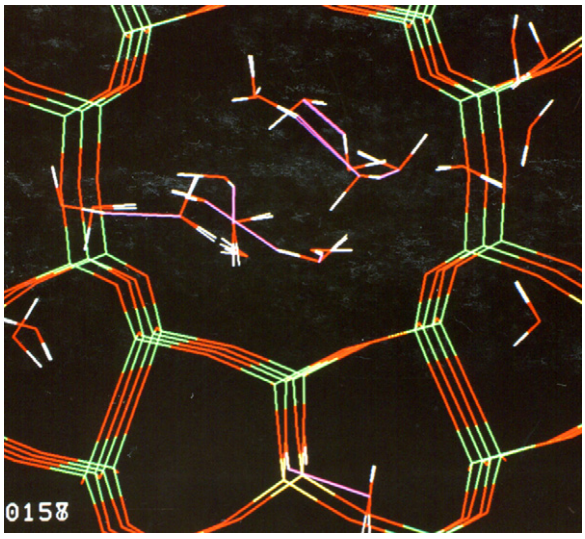

Fig. 13. Snapshot from an MD simulation of water molecules inside H-ferrierite, depicting the formation of the water cage structure in the main channel of the framework. Pink lines depict the H-bonds among the water molecules in the main channel or with the hydrogen framework atoms (For interpretation of the references to color in this figure legend, the reader is referred to the web version of the article).

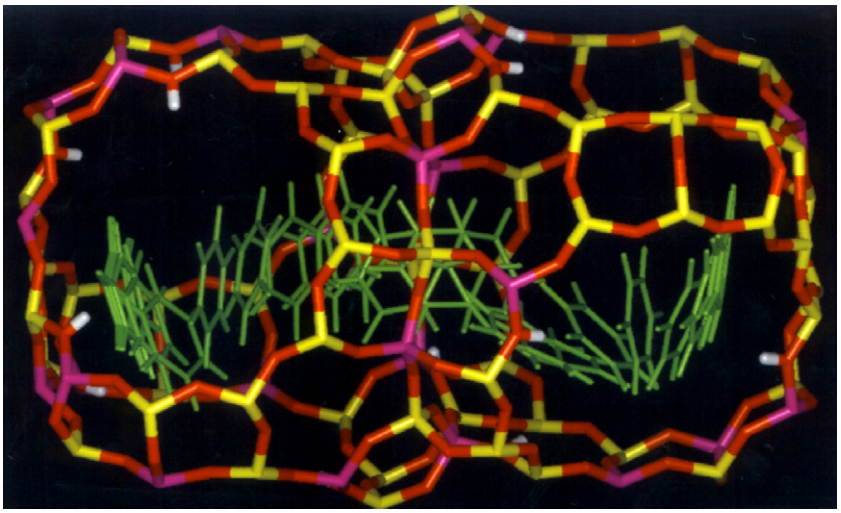

Fig. 14. Successive positions of a benzene molecule creeping in the channel of zeolite HY, obtained from MD simulations.

rate representation of the electric field and its derivatives. Such detailed studies were performed by some of us (A.L. and D.P.V.) considering 3D periodic zeolite models at different levels of theory, i.e., Hartree–Fock [27] and DFT [28]. The convergence of the electric field in all-siliceous and H-form zeolites at the DFT/B3LYP level [29–30] allowed confirming the accuracy of the earlier computations [25–26].

More recently, two of us (M.E. and D.P.V.) went on to the important problem of helping to the syntheses of molecular sieves. The principles governing the formation of crystalline porous materials are indeed not yet well understood, despite the great efforts made, because of the complexity of the hydrothermal crystallizations [31]. It is known that a good fit between the organic template and the host framework is necessary [32]. However, as for example in the case of $AlPO_4$-5, which attracted much of interest due to its applications in materials science and catalysis. the experimental observations, *multiple-templates-one-structure and one-template-multiple-structures*, cannot yet be clearly explained; $AlPO_4$-5 can be prepared using more than 25 different templates [33]. In conjunction with experimental characterization (XRD, TG, FT-Raman, and SEM), non-bonding interaction energies regarding several templates, i.e., methyldicyclohexylamine (MCHA), triethylamine (TEA), tripropylamine (TPA), or tetraethylammonium hydroxide (TEAOH), optimized inside the $AlPO_4$-5 framework were calculated at the density functional theory (DFT) level considering periodic conditions, using DMol^3 (Fig. 15) [34]. In those studies, it was shown

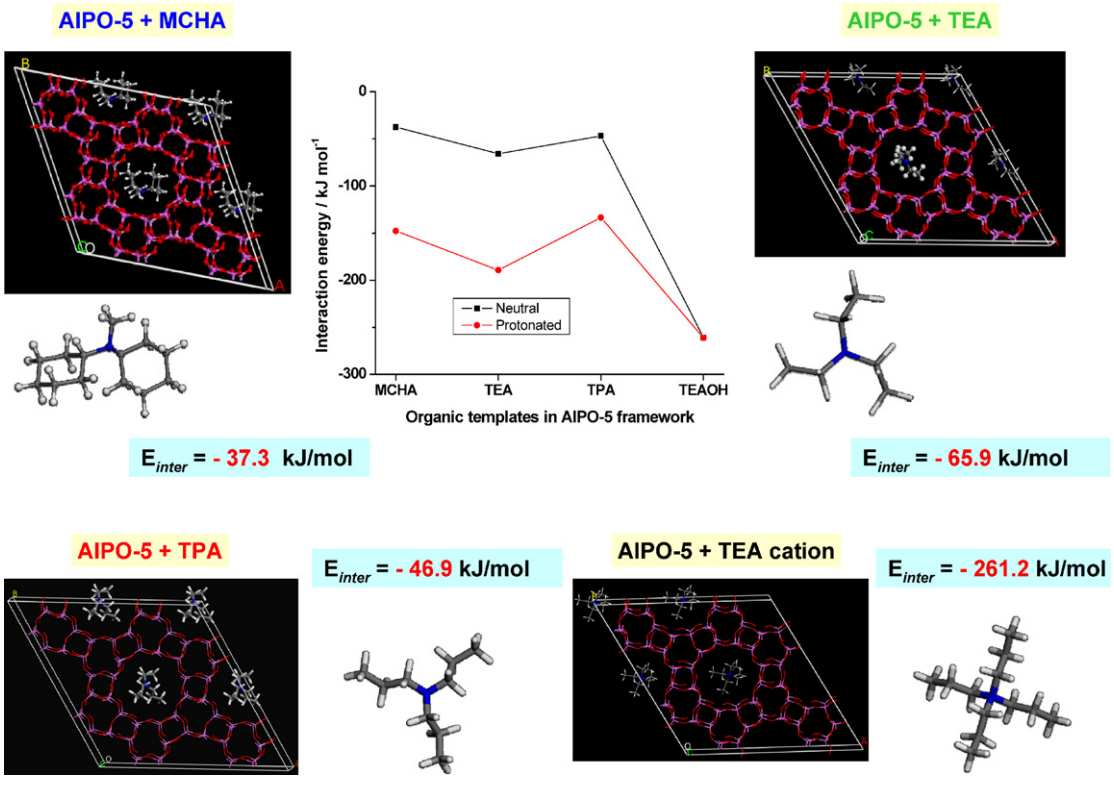

Fig. 15. Fully optimized structures of $AlPO_4$-5 (super-cells $2 \times 2 \times 2$) occluding different organic templates used in the synthesis of $AlPO_4$-5, and non-bonding interaction energy between the template and the framework as obtained from periodic DFT calculations with DMol^3.

that TEAOH has the best ability to form the $AlPO_4$-5 structure as compared with other templates. Characterizing fully the $AlPO_4$-5 framework occluding the various organic templates is thus expected to give a better insight into the confinement of organic templates in a porous framework and its role in directing the synthesis and topology of the produced crystals.

Acknowledgments

All authors wish to acknowledge all their colleagues, theoreticians or experimentalists from both the Physics and Chemistry Departments, who have participated as co-authors of the numerous FUNDP papers on confinement in general. The authors also thank the FUNDP, the FNRS-FRFC, and the Loterie Nationale (convention 2.4578.02 and earlier) for the use of the Namur Interuniversity Scientific Computing Facility (iSCF). M.E. thanks the FNRS for his Post-Doctoral fellowship.

References

[1] M. Schmeits, A.A. Lucas, J. Chem. Phys. 65 (1976) 2901.
[2] E.G. Derouane, J.-M. André, A.A. Lucas, Chem. Phys. Lett. 137 (1987) 336.
[3] E.G. Derouane, J. B'Nagy, Chem. Phys. Lett. 137 (1987) 341.
[4] E.G. Derouane, Chem. Phys. Lett. 142 (1987) 200.
[5] E.G. Derouane, J.-M. André, A.A. Lucas, J. Catal. 110 (1988) 58.
[6] E.G. Derouane, J. B'Nagy, Ch. Fernandez, Z. Gabelica, E. Laurent, P. Maljean, Appl. Catal. 40 (1988) Ll.
[7] Ph. Lambin, A.A. Lucas, I. Derycke, J.-P. Vigneron, E.G. Derouane, J. Chem. Phys. 90 (1989) 3814.
[8] E.G. Derouane, L. Leherte, D.P. Vercauteren, A.A. Lucas, J.-M. André, J. Catal. 119 (1989) 266.
[9] I. Derycke, J.-P. Vigneron, Ph. Lambin, A.A. Lucas, E.G. Derouane, J. Chem. Phys. 94 (1991) 4620.
[10] J.H. de Boer, J.F. Custers, Z. Phys. Chem. B 25 (1934) 225.
[11] M. Legros, G. Dehm, E. Arzt, T.J. Balk, Science 319 (2008) 1646.
[12] E.G. Derouane, D.J. Vanderveken, Appl. Catal. 45 (1988) L15.
[13] E.G. Derouane, J. B'Nagy, Appl. Catal. 52 (1989) 169.
[14] E.G. Derouane, Zeolites 13 (1993) 67.
[15] E.G. Derouane, Appl. Catal. 115 (1994) N2.
[16] E.G. Derouane, J. Mol. Catal. A 134 (1998) 29.
[17] E.G. Derouane, C.D. Chang, Microporous Mesoporous Mater. 35–36 (2000) 425.
[18] E.G. Derouane, Microporous Mesoporous Mater. 104 (2007) 46.
[19] D.P. Vercauteren, L. Leherte, D.J. Vanderveken, J.A. Horsley, C.M. Freeman, E.G. Derouane, in: R.W. Joyner, R.A. Van Santen (Eds.), Elementary Reaction Steps in Heterogeneous Catalysis, Kluwer Academic Publishers, Dordrecht, 1993, pp. 389–401.
[20] L. Leherte, J.-M. André, E.G. Derouane, D.P. Vercauteren, Int. J. Quantum Chem. 42 (1992) 1291 (and references therein).
[21] F. Jousse, S.M. Auerbach, D.P. Vercauteren, J. Phys. Chem. B 102 (1998) 6507 (and references therein).
[22] C. Hansenne, F. Jousse, L. Leherte, D.P. Vercauteren, J. Mol. Catal. A 166 (2001) 147 (and references therein).
[23] S.M. Auerbach, F. Jousse, D.P. Vercauteren, in: C.R.A. Catlow, R.A. van Santen, B. Smit (Eds.), Computer Modelling of Microporous Materials, Elsevier-Academic Press, Amsterdam, 2004, pp. 49–108 (and references therein).
[24] K.S. Smirnov, F. Thibault-Starzyk, J. Phys. Chem. B 103 (1999) 8595.
[25] A.V. Larin, L. Leherte, D.P. Vercauteren, Phys. Chem. Chem. Phys. 4 (2002) 2416.
[26] A.V. Larin, D.P. Vercauteren, C. Lamberti, S. Bordiga, A. Zecchina, Phys. Chem. Chem. Phys. 4 (2002) 2424.
[27] A.V. Larin, D.P. Vercauteren, Int. J. Quantum Chem. 83 (2001) 70.
[28] A.V. Larin, V.S. Parbuzin, D.P. Vercauteren, Int. J. Quantum Chem. 101 (2005) 807.
[29] A.V. Larin, D.N. Trubnikov, D.P. Vercauteren, Int. J. Quantum Chem. 107 (2007) 3137.
[30] A.V. Larin, D.N. Trubnikov, D.P. Vercauteren, J. Comp. Chem. 29 (2008) 130.
[31] C.S. Cundy, P.A. Cox, Microporous Mesoporous Mater. 82 (2005) 1.
[32] D.W. Lewis, in: C.R.A. Catlow, R.A. van Santen, B. Smit (Eds.), Computer Modelling of Microporous Materials, Elsevier-Academic Press, Amsterdam, 2004, pp. 243–265 (and references therein).
[33] J.H. Yu, R.R. Xu, Chem. Soc. Rev. 35 (2006) 593.
[34] M. Elanany, B.-L. Su, D.P. Vercauteren, J. Mol. Catal. A 270 (2007) 295 (and references therein).